THE ELECTRIC FIELD OF AN IDEALIZED DEE GEOMETRY AND ITS EFFECTS ON CYCLOTRON ORBIT PROPERTIES

Thesis for the Degree of M. S.

MICHIGAN STATE UNIVERSITY

Jack W. Beal

1962

ABSTRACT

THE ELECTRIC FIELD OF AN IDEALIZED DEE GEOMETRY AND ITS EFFECTS ON CYCLOTRON ORBIT PROPERTIES

by Jack W. Beal

An analytic solution for the electric field and potential due to an idealized cyclotron dee geometry is rederived using the Schwarz-Christoffel transformation. The general results obtained in this manner are reduced according to the median plane requirement. Using the derived results for the median plane electric field and potential, MISTIC is used to determine particle orbits and properties of these orbits. Good agreement is obtained between computer results and direct, non-relativistic calculations. The questions of radial stability and isochronism are investigated pertinent to locating the optimum particle source position. The results of the stability consideration are qualitatively verified on the basis of orbit centering.

Morton M. Gordon

THE ELECTRIC FIELD OF AN IDEALIZED DEE GEOMETRY AND ITS EFFECTS ON CYCLOTRON ORBIT PROPERTIES

By

Jack W. Beal

A THESIS

Submitted to
Michigan State University
in partial fulfillment of the requirements
for the degree of

MASTER OF SCIENCE

Department of Physics and Astronomy

1962

ACKNOWLEDGMENTS

I would like to express my appreciation to Dr. M. M. Gordon and Dr. H. G. Blosser of this laboratory. Without their many helpful suggestions and discussions this work would not have been completed.

I would extend my thanks to T. I. Arnette, D. A. Johnson and S. L. Steinberg for their helpful work with computer problems.

Also, my thanks to R. L. Dickenson for his work on the figures and drawings.

TABLE OF CONTENTS

LIST OF TABLES

LIST OF FIGURES

INTRODUCTION

This report is divided into two main sections. The first section presents an analytic derivation to calculate electric fields and potentials within an idealized cyclotron dee geometry. The second section deals with computation of ion trajectories within the idealized cyclotron using results of the previously determined electric fields and potentials and using a three-sector magnetic field of the form contemplated for the MSU 64" cyclotron.

In any complete analysis of ion trajectories in a cyclotron, data as to the magnitude and shape of the electric field and potential are necessary. There have been several methods presented by investigators to determine the electric field intensities. For example, R. R. Wilson [1]* used data obtained from electrolytic models. M. E. Rose [2] used special properties of the conjugate functions that represent field and potential lines; while Bohm and Foldy [3] assumed uniformity in the dee gap. This paper presents again an analytical method of determining the electric fields and potentials by use of the Schwarz-Christoffel transformation. This derivation, due originally to R. L. Murray and L. T. Ratner [4], is presented

---

*References will be given in square brackets and all references will be listed at the end of this report.

again in order to correct typographical errors in their report. Using the equations resulting from the derivation, values of the electric field and potential can be calculated for points within the cyclotron dees.

Using the computational method for electric fields and potentials, it is then possible to completely determine particle orbits through the idealized cyclotron. A MISTIC computer program named Cartwheel [5] is used to make this determination. By comparing Cartwheel results for the uniform electric field and derived electric field, information is obtained to determine the effects of the electric field on the particle orbits. These results are presented and discussed in the final sections of this work.

I. ELECTRIC FIELD AND POTENTIAL CALCULATIONS

A. Derivation of General Results

The dee geometry assumed is shown in Fig. 1-1. This geometry consists of two parallel conducting planes, each located at a distance h from the x-y median plane and with a y separation of width 2k oriented along the x axis.

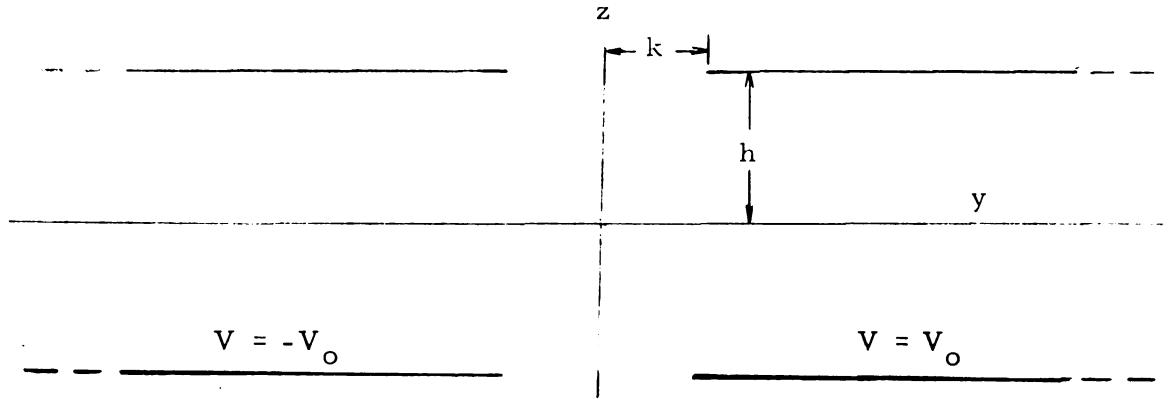

Fig. 1-1. Cyclotron Dee Geometry.

The right and left dee segments are chosen to be at $V = V_o$ and $V = -V_o$ respectively; therefore, the x-z plane, the plane of symmetry, is at $V = 0$. Also, from symmetry considerations, there is no electric field component in the x direction. Hence, the dee geometry is idealized and is thereby reduced to a simple two-dimensional geometry. It is important to note that in this idealization, the effect of the cyclotron

liner has been neglected. It is expected that this is a good approximation for small k values, while the results for large k will be rather inconsistent with the actual cyclotron. Also, edge effects due to the finite size of the dees has been neglected.

Following Murray and Ratner, by use of the Schwarz-Christoffel transformation [6], it is possible to map the region for which the fields and potentials are unknown to one for which the fields and potentials are obvious such as the fields and potentials due to two parallel conducting planes. For the purposes of this mapping, the transformation is performed in terms of the complex parameter t. Fig. 1-2 shows the w-plane and the one-to-one correspondence as it is mapped to the upper half of the t-plane. The symmetry about the z-axis is here being employed as only one-half of the entire dee geometry is being mapped.

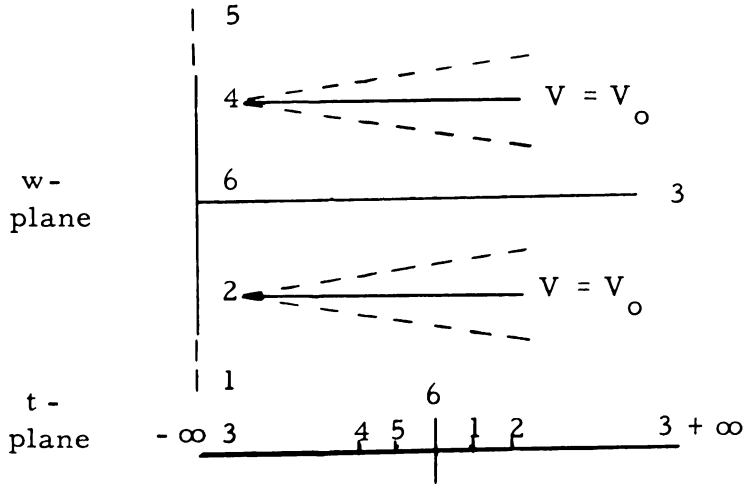

Fig. 1-2. Transformation from w-plane to t-plane.

The function which maps the real axis of the t-plane into the polygon of the w-plane is then given by the Schwarz-Christoffel equation

$$w = C \int \prod_{i=1} (t-t_i)^{\frac{\alpha_i}{\pi} - 1} dt, \tag{1.1}$$

where the α_i's are the interior angles of the polygon in the w-plane. The angles, α_i, of the polygon and values of real t corresponding to vertices in the w-plane as shown in Fig. 1-2 are tabulated below.

i	t_i	α_i
1	a	$-\pi/2$
2	1	2π
3	$\pm\infty$	0
4	-1	2π
5	-a	$-\pi/2$
6	0	π

The value of a is to be determined from the boundary conditions. Substitution of these values into Eq. (1.1) yields

$$w = C\left[\int \frac{t^2 dt}{(t^2-a^2)^{3/2}} - \int \frac{dt}{(t^2-a^2)^{3/2}}\right]. \tag{1.2}$$

Integrating Eq. (1. 2) and using the identity $\log\left(t + \sqrt{t^2-a^2}\right) = \cosh^{-1}\left(\frac{t}{a}\right) + \log a$, the transformation equation is

$$w = C\left[\cosh^{-1}\left(\frac{t}{a}\right) + \log a + \frac{1-a^2}{a^2}\,\frac{t}{\sqrt{t^2-a^2}}\right] + K, \qquad (1.3)$$

where K is a constant of integration.

In order to evaluate the three constants C, K and a of Eq. (1. 3), the boundary conditions are applied; that is, $w = 0$ at $t = 0$ and $w = k - ih$ at $t = 1$. Thus for $w = 0$ at $t = 0$, Eq. (1. 3) reduces to

$$K = -C\left(\pm i\pi/2 + \log a\right).$$

At the secondary boundary point $w = k - ih$ at $t = 1$, therefore, Eq. (1. 3) yields

$$k - ih = C\left[\cosh^{-1}\left(\frac{1}{a}\right) + \log a + \sqrt{\frac{1-a^2}{a^2}}\right] + K.$$

Substituting for K from above gives

$$k - ih = C\left[\cosh^{-1}\left(\frac{1}{a}\right) + \log a + \sqrt{\frac{1-a^2}{a^2}} \mp \frac{i\pi}{2} - \log a\right].$$

Choosing the negative sign for the constant term $\frac{i\pi}{2}$ inside the bracket, in other words, considering negative y values, and equating imaginary parts, C is determined, $C = \frac{2h}{\pi}$. Equating real parts, a is determined by the equation

$$\frac{\pi k}{2h} = \cosh^{-1}\left(\frac{1}{a}\right) + \frac{\sqrt{1-a^2}}{a^2} \quad . \tag{1.4}$$

Therefore, the equation of the transformation, correct for negative y, becomes

$$w = \frac{2h}{\pi}\left[\cosh^{-1}\left(\frac{t}{a}\right) + \frac{1-a^2}{a^2}\,\frac{t}{\sqrt{t^2-a^2}} - i\pi/2\right] , \tag{1.5}$$

Now to consider the transformation from a region for which the fields and potentials are known again to the upper half of the t-plane. Fig. 1-3 shows the polygon which may be used to map the region between two infinite planes, for which the electric field is linear, onto the upper half of the t-plane.

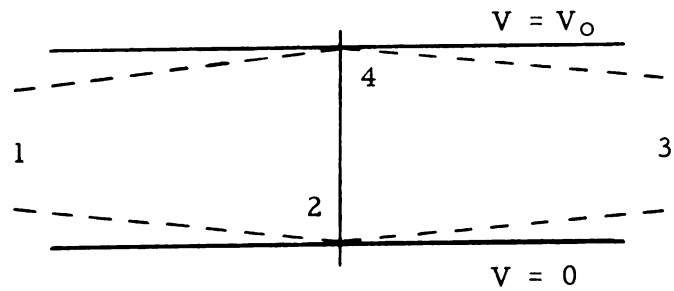

Fig. 1-3. Polygon for Mapping Strip into Half Plane.

The angles, β_i, of the polygon in the W-plane and the values of real t corresponding to vertices in W space as shown in Fig. 1-3 are tabulated below.

i	t_i	β_i
1	-a	0
2	0	π
3	+a	0
4	$\pm\infty$	π

Substitution of these values into Eq. (1.1) yields

$$W = D\int \frac{dt}{t^2 - a^2} .$$

Integrating the above yields

$$W = U + iV = -\frac{D}{a} \tanh^{-1}\left(\frac{t}{a}\right) + E. \qquad (1.6)$$

Applying the boundary conditions, $t = 0$ at $W = 0$ and $t = \pm\infty$ at $W = iV_o$ in order to evaluate the constants in Eq. (1.6), the results are

$$0 = -\frac{D}{a}\tanh^{-1}(0) + E,$$

and

$$iV_o = -\frac{D}{a}\tanh^{-1}(\pm\infty) + E.$$

Hence, $E = 0$ and $D = -\frac{2V_o a}{\pi}$ are the values of the constants. Therefore, the transformation equation from the W-plane to the t-plane is given by

$$W = U + iV = \frac{2V_o}{\pi} \tanh^{-1}\frac{t}{a} .$$

For ease of notation, let $u = \frac{\pi U}{2V_o}$ and $v = \frac{\pi V}{2V_o}$, therefore

$$\tanh^{-1}\frac{t}{a} = u + iv = S,$$

or

$$\frac{t}{a} = \tanh S. \tag{1.7}$$

Now having a parameter representation for the transformation, Eq. (1.7) can be substituted into Eq. (1.5) giving the result

$$w = \frac{2h}{\pi}\left[\cosh^{-1}(\tanh S) + \left(\frac{1-a^2}{a^2}\right)\frac{\tanh S}{\sqrt{\tanh^2 S - 1}} - \frac{i\pi}{2}\right].$$

Using the identity $\cosh^{-1} x = \log\left(x + \sqrt{x^2 - 1}\right)$, the above equation can be written

$$w = \frac{2h}{\pi}\left[\log(\tanh S \pm i\,\mathrm{sech}\, S) \mp i\left(\frac{1-a^2}{a^2}\right)\sinh S - \frac{i\pi}{2}\right].$$

By checking the case $w = 0$, the ambiguity in signs can be resolved to give the transformation equation in the form

$$w = \frac{2h}{\pi}\left[\log(\tanh S + i\,\mathrm{sech} S) - i\left(\frac{1-a^2}{a^2}\right)\sinh S - \frac{i\pi}{2}\right]. \tag{1.8}$$

The transformation equation must now be separated into real and imaginary parts to determine $y = y(S)$ and $z = z(S)$, recalling that $w = y + iz$ and $S = u + iv$. This process is tedious but straightforward.

First, the term of the form $\log(a + ib)$ is rationalized; that is

$$\log(a + ib) = M + iN,$$

or

$$a + ib = e^{M}(\cos N + i\sin N),$$

therefore

$$N = \tan^{-1}\left(\frac{b}{a}\right),$$

and

$$M = \frac{1}{2}\log(a^2 + b^2).$$

Rewriting Eq. (1.8)

$$w = \frac{2h}{\pi}\left[\log(\sinh S + i) - \log\cosh S - i\left(\frac{1-a^2}{a^2}\right)\sinh S - \frac{i\pi}{2}\right],$$

and applying the above rationalization technique, yields

$$w = \frac{2h}{\pi}\left[i\tan^{-1}\left(\frac{1}{\sinh S}\right) - i\left(\frac{1-a^2}{a^2}\right)\sinh S - \frac{i\pi}{2}\right],$$

$$= \frac{2h}{\pi}\left\{\frac{1}{2}\log\left[\frac{\sinh(u+iv) + i}{\sinh(u+iv) - i}\right] - \frac{i}{A}(\sinh u\cos v + i\cosh u\sin v) - \frac{i\pi}{2}\right\},$$

where $A = \dfrac{a^2}{1-a^2}$.

Again applying the previous rationalization to the terms of the form $\log(a+ib)$ and straightforwardly simplifying the real and imaginary parts of the rationalization by using standard trigonometric identities, the result is

$$w = y + iz = \frac{2h}{\pi}\left[\tanh^{-1}\left(\frac{\sin v}{\cosh u}\right) - i\tan^{-1}\left(\frac{\sinh u}{\cos v}\right) - \frac{i}{A}\sinh u\cos v + \frac{1}{A}\cosh u\sin v\right].$$

Letting $Y = \frac{\pi y}{2h}$ and $Z = \frac{\pi z}{2h}$ and writing real and imaginary parts, then

$$Y = \tanh^{-1}\left(\frac{\sin v}{\cosh u}\right) + \frac{1}{A}\cosh u \sin v, \tag{1.9a}$$

$$-Z = \tan^{-1}\left(\frac{\sinh u}{\cos v}\right) + \frac{1}{A}\sinh u \cos v. \tag{1.9b}$$

The electric fields desired are determined by $E_y = \frac{\partial V}{\partial y}$ and $E_z = \frac{\partial V}{\partial z}$. However, Eqs. (1.9) above give Y(u, v) and Z(u, v). Using the Cauchy-Riemann conditions, $\frac{\partial U}{\partial y} = \frac{\partial V}{\partial z}$ and $\frac{\partial U}{\partial z} = -\frac{\partial V}{\partial y}$, differentiation of Eq. (1.9a) above with respect to y gives

$$\frac{V_o}{h} = \frac{\partial Y}{\partial u} E_z + \frac{\partial Y}{\partial v} E_y. \tag{1.10a}$$

Differentiating Eq. (1.9a) with respect to z and applying the Cauchy-Riemann condition yields

$$0 = -\frac{\partial Y}{\partial u} E_y + \frac{\partial Y}{\partial v} E_z. \tag{1.10b}$$

Solving the Eqs. (1.10) simultaneously for E_y and E_z gives the results for the electric fields

$$E_y = \frac{V_o}{h}\left[\frac{Y_v}{Y_v^2 + Y_u^2}\right], \tag{1.11a}$$

$$E_z = \frac{V_o}{h}\left[\frac{Y_{u'}}{Y_v^2 + Y_u^2}\right]. \tag{1.11b}$$

The derivatives Y_u and Y_v are determined

$$Y_u = \sinh u \sin v\left[\frac{1}{A} - \frac{1}{\cosh^2 u - \sin^2 v}\right], \tag{1.12a}$$

$$Y_v = \cosh u \cos v\left[\frac{1}{A} + \frac{1}{\cosh^2 u - \sin^2 v}\right]. \tag{1.12b}$$

Therefore, use of Eqs. (1.11) coupled with Eqs. (1.12) will determine the electric fields within the cyclotron dees. However, these equations are still functions of u and v; therefore, a computation method is developed to determine the fields as a function of position.

In order to facilitate the computational studies, it is best to rewrite Eqs. (1.9) as

$$Y = Y_1 + \Delta Y,$$

$$-Z = Z_1 + \Delta Z,$$

where

$$\Delta Y = \frac{1}{A} \cosh u \sin v,$$

$$\Delta Z = \frac{1}{A} \sinh u \cos v,$$

$$Y_1 = \tanh^{-1} \left(\frac{\sin v}{\cosh u}\right),$$

$$Z_1 = \tan^{-1} \left(\frac{\sinh u}{\cos v}\right).$$

Now it is possible to express functions of u and v in terms of functions of Y and Z. For example, $\tanh Y_1 = \frac{\sin v}{\cosh u}$ and $\tan Z_1 = \frac{\sinh u}{\cos v}$ or $\cosh u = \frac{\sin v}{\tanh Y_1}$ and $\sinh u = \cos v \tan Z_1$. Using the trigonometric identity $\cosh^2 a - \sinh^2 a = 1$, the above relations for coshu and sinhu lead to the equation

$$\frac{\sin^2 v}{\tanh^2 Y_1} - \cos^2 v \tan^2 Z_1 = 1.$$

After rearrangement using the identity $\cosh^2 a \cos^2 b + \sinh^2 a \sin^2 b = \cosh^2 a - \sin^2 b$, the result is

$$\sin v = \frac{\sinh Y_1}{F}, \qquad (1.13a)$$

where $F^2 = (\cosh^2 Y_1 - \sin^2 Z_1)$.

By similar treatments

$$\cos v = \frac{\cos Z_1}{F}, \qquad (1.13b)$$

$$\text{sinhu} = \frac{\sin Z_1}{F}, \tag{1.13c}$$

$$\text{coshu} = \frac{\cosh Y_1}{F}. \tag{1.13d}$$

Substitution of these quantities into Eqs. (1.12), the derivative relations, yields

$$Y_v = \cosh Y_1 \cos Z_1 \left(1 + \frac{1}{AF^2}\right), \tag{1.14a}$$

$$Y_u = -\sinh Y_1 \sin Z_1 \left(1 - \frac{1}{AF^2}\right), \tag{1.14b}$$

Also, by substitution, Eqs. (1.9) can be written

$$Y = Y_1 + \frac{\sinh Y_1 \cosh Y_1}{AF^2}, \tag{1.15a}$$

$$-Z = Z_1 + \frac{\sin Z_1 \cos Z_1}{AF^2}. \tag{1.15b}$$

Eqs. (1.13a) and (1.13b) above can be used to determine the potential v. The resultant equations for v are

$$v = \sin^{-1}\left[\frac{\sinh Y_1}{F}\right], \tag{1.16a}$$

$$v = \pm \cos^{-1}\left[\frac{\cos Z_1}{F}\right], \ (\pm y). \tag{1.16b}$$

In Eqs. (1.11) given above to calculate the electric fields and in Eqs. (1.16) to calculate the potentials, the fields and potentials are explicit functions of Y_1 and Z_1 rather than the space coordinates Y and Z. Therefore, the quantities Y_1 and Z_1 must be determined for a given Y and Z by the transcendental equations, Eqs. (1.15), as given. Therefore, the procedure of Eqs. (1.15) coupled with Eqs. (1.11) and Eqs. (1.16) can be used to determine the electric field and potential at a point (Y, Z) within the dee region.

B. Summary of General Results

Presented below are the equations for electric field, potential, and computation method for the general case derived above.

$$E_y = \frac{V_o}{h}\left[\frac{Y_v}{Y_v^2 + Y_u^2}\right], \tag{1.11a}$$

$$E_z = \frac{V_o}{h}\left[\frac{Y_u}{Y_v^2 + Y_u^2}\right], \tag{1.11b}$$

$$Y_v = \cosh Y_1 \cos Z_1 \left(1 + \frac{1}{AF^2}\right), \tag{1.14a}$$

$$Y_u = -\sinh Y_1 \sin Z_1 \left(1 - \frac{1}{AF^2}\right), \tag{1.14b}$$

$$A = \frac{a^2}{1-a^2}\ ,\quad F^2 = \cosh^2 Y_1 - \sin^2 Z_1,$$

$$\frac{\pi}{2}\frac{k}{h} = \cosh^{-1}\left(\frac{1}{a}\right) + \frac{\sqrt{1-a^2}}{a^2}\ , \tag{1.4}$$

$$Y = Y_1 + \frac{\sinh Y_1 \cosh Y_1}{AF^2}\ , \tag{1.15a}$$

$$-Z = Z_1 + \frac{\sin Z_1 \cos Z_1}{AF^2}\ , \tag{1.15b}$$

$$Y = \frac{\pi}{2}\frac{y}{h},\quad Z = \frac{\pi}{2}\frac{z}{h}$$

$$v = \frac{\pi}{2}\frac{V}{V_o}\ ,\quad u = \frac{\pi}{2}\frac{U}{V_o},$$

$$v = \sin^{-1}\left[\frac{\sinh Y_1}{F}\right], \tag{1.16a}$$

$$v = \pm\cos^{-1}\left[\frac{\cos Z_1}{F}\right],\quad (\pm y). \tag{1.16b}$$

C. Median Plane Results

For the present, for use in conjunction with Cartwheel, to be discussed in later sections, the electric fields and potentials of interest were those of the median plane ($z = 0$). This specification simplifies

the preceding equations for the electric field, potential and computation calculations. The results are

$$E_y = \frac{V_o}{h}\left[\frac{\operatorname{sech} Y_1}{1 + \frac{1}{A}\operatorname{sech}^2 Y_1}\right], \tag{1.17a}$$

$$E_z = 0, \tag{1.17b}$$

$$v = \pm \cos^{-1}\left[\operatorname{sech} Y_1\right], \quad (\pm y) \tag{1.17c}$$

$$Y = Y_1 + \frac{1}{A}\tanh Y_1, \tag{1.17d}$$

$$Z = 0$$

These equations for electric fields and potentials are well behaved and relatively simple to use.

The transcendental equation, Eq. (1.17d), for the calculation of Y_1 converges slowly for small values of $\frac{1}{A}$ and does not converge at all for large $\frac{1}{A}$. However, the following iteration process was developed and was found to work well in all cases.

First, assume that Y_1^* is an approximate solution to Eq. (1.17d) above such that $(Y_1 - Y_1^*)$ is small. Expanding $\tanh Y_1$ in Eq. (1.17d) to first order in $(Y_1 - Y_1^*)$, and solving for Y_1 the result is

$$Y_1 = \frac{Y - \frac{1}{A}\tanh Y_1^* + \frac{1}{A} Y_1^* \operatorname{sech}^2 Y_1^*}{1 + \frac{1}{A}\operatorname{sech}^2 Y_1^*} \tag{1.18}$$

The iteration process then consists of taking an initial guess for Y_1, setting this equal to Y_1^* on the right and solving for Y_1; then, taking this new value for Y_1 and setting it equal to Y_1^* on the right again solving for Y_1 repeating this process until the difference in successive values of Y_1 is sufficiently small. The iteration is such that if a given Y_1^* has an error of order ϵ, then Y_1 given by Eq. (1.18) will have an error of order ϵ^2.

In order for the iteration process to work efficiently it is necessary to determine a reasonable guess for the initial value of Y_1. To obtain such a guess it need only be noted that since $\tanh Y_1 \leq Y_1$ for small Y_1, then $Y_1 \geq Y/(1 + \frac{1}{A})$ for Y_1 small; and since $\tanh Y_1 \leq 1$ for large Y_1, then $Y_1 \geq Y - \frac{1}{A}$ for Y_1 large. A simple choice for the initial value of Y_1 is then

$$Y_1 = Y/(1 + \frac{1}{A}) \text{ for } 1 + 1/A > Y \tag{1.19a}$$

$$Y_1 = Y - \frac{1}{A} \quad \text{for } 1 + 1/A \leq Y \tag{1.19b}$$

For the case $Y = 1 + 1/A$ either of Eqs. (1.19) yields the same value of Y_1. With this choice for the initial value, the iteration procedure described works well for all values of $\frac{1}{A}$. This method can be

extended to the general iteration procedure of Eqs. (1.15) for the case of large $\frac{1}{A}$.

At this point it would be well to note some results for the calculation of electric fields and potentials before turning to the determination of particle orbits obtained in using these fields. A fixed point computer program for use on MISTIC was used to perform the indicated operations in the median plane equations given above. Values of E_y and V_y at the points (Y, 0) with $\frac{1}{A} < 4$ were obtained. Fig. 1-4 shows the electric field in the y direction for two gap dimension parameters, and Fig. 1-5 shows the associated potential for the same dee gap arrangements. Table I gives values of electric field and potential for a wide range of dee gap parameters. These curves and the table of values exhibit the predominant variations of the electric field and potential as a function of position in the median plane and also as a function of dee gap geometry.

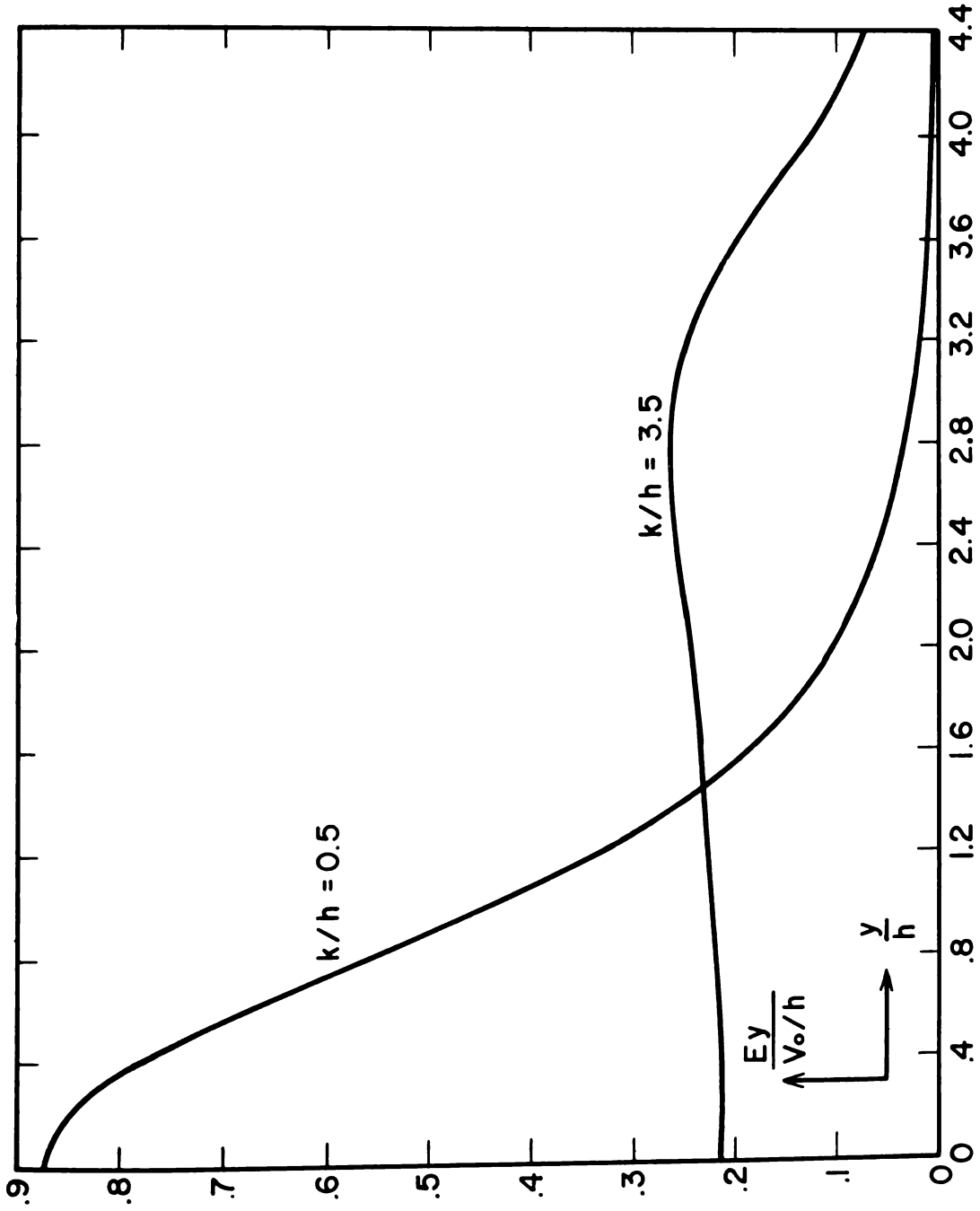

Fig. 1-4. Median Plane Electric Field vs. Position for Two Gap Parameters, Sec. C, Fig. 1-1.

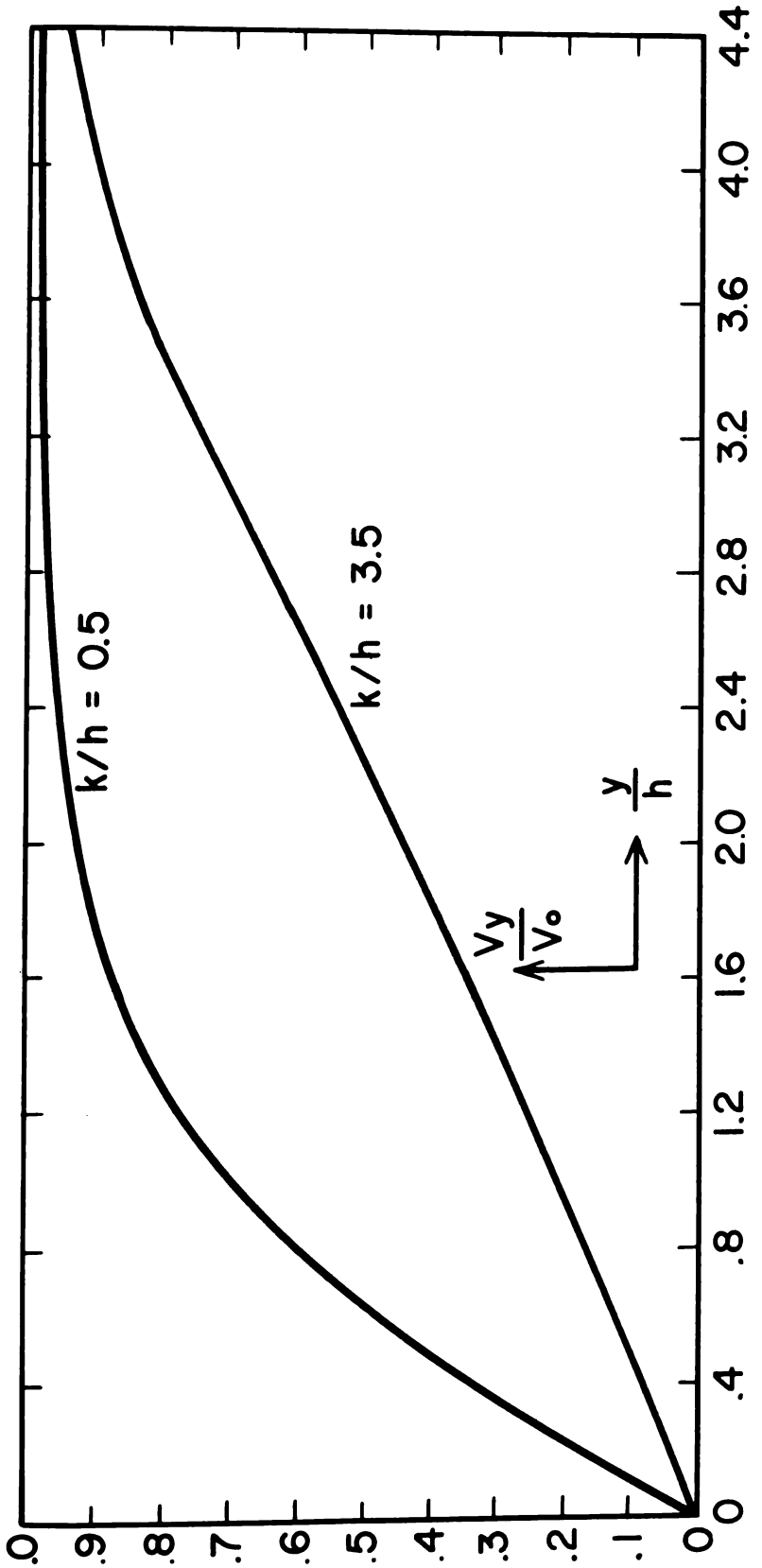

Fig. 1-5. Median Plane Potential vs. Position for Two Gap Parameters, Sec.C, Fig. 1-1.

Table I

Median Plane Electric Field and Potential for Various Dee Gap Parameters Sec. C

$\frac{k}{h} = 0.1$

$\frac{y}{h}$	$\frac{E}{V_o/h}$	$\frac{V}{V_o}$
0.00	0.99388	0.00000
0.20	0.94784	0.19566
0.40	0.82863	0.37420
0.60	0.67692	0.52496
0.80	0.52800	0.64520
1.00	0.40021	0.73760
1.20	0.29834	0.80702
1.40	0.22033	0.85853
1.60	0.16189	0.89647
1.80	0.11862	0.92430
2.00	0.08679	0.94468
2.20	0.06345	0.95958
2.40	0.04637	0.97047
2.60	0.03388	0.97843
2.80	0.02475	0.98424
3.00	0.01808	0.98849
3.20	0.01320	0.99159
3.40	0.00964	0.99386
3.60	0.00704	0.99551
3.80	0.00515	0.99672
4.00	0.00376	0.99760
4.20	0.00274	0.99825
4.40	0.00200	0.99872
4.60	0.00146	0.99906
4.80	0.00107	0.99931
5.00	0.00078	0.99950

Table I (Cont.)

$\frac{k}{h} = 0.3$

$\frac{y}{h}$	$\frac{E}{V_o/h}$	$\frac{V}{V_o}$
0.00	0.94834	0.00000
0.20	0.91160	0.18719
0.40	0.81244	0.36044
0.60	0.67821	0.50983
0.80	0.53843	0.63138
1.00	0.41305	0.72618
1.20	0.31019	0.79811
1.40	0.23005	0.85178
1.60	0.16943	0.89144
1.80	0.12431	0.92059
2.00	0.09101	0.94196
2.20	0.06656	0.95759
2.40	0.04865	0.96902
2.60	0.03555	0.97737
2.80	0.02597	0.98347
3.00	0.01897	0.98792
3.20	0.01386	0.99118
3.40	0.01012	0.99355
3.60	0.00739	0.99529
3.80	0.00540	0.99656
4.00	0.00394	0.99748
4.20	0.00288	0.99816
4.40	0.00210	0.99866
4.60	0.00154	0.99902
4.80	0.00112	0.99928
5.00	0.00082	0.99947

Table I (Cont.)

$\frac{k}{h} = 0.5$

$\frac{y}{h}$	$\frac{E}{V_o/h}$	$\frac{V}{V_o}$
0.00	0.87049	0.00000
0.20	0.84658	0.17250
0.40	0.77779	0.33562
0.60	0.67446	0.48129
0.80	0.55436	0.60429
1.00	0.43639	0.70319
1.20	0.33326	0.77985
1.40	0.24966	0.83781
1.60	0.18492	0.88098
1.80	0.13610	0.91285
2.00	0.09982	0.93626
2.20	0.07307	0.95341
2.40	0.05343	0.96596
2.60	0.03905	0.97513
2.80	0.02853	0.98183
3.00	0.02084	0.98673
3.20	0.01523	0.99030
3.40	0.01112	0.99292
3.60	0.00812	0.99483
3.80	0.00593	0.99622
4.00	0.00433	0.99724
4.20	0.00317	0.99798
4.40	0.00231	0.99852
4.60	0.00169	0.99892
4.80	0.00123	0.99921
5.00	0.00090	0.99942

Table I (Cont.)

$\frac{k}{h} = 1.0$

$\frac{y}{h}$	$\frac{E}{V_o/h}$	$\frac{V}{V_o}$
0.00	0.65448	0.00000
0.20	0.65008	0.13061
0.40	0.63538	0.25935
0.60	0.60647	0.38381
0.80	0.55908	0.50070
1.00	0.49250	0.60615
1.20	0.41267	0.69680
1.40	0.33033	0.77105
1.60	0.25529	0.82943
1.80	0.19269	0.87401
2.00	0.14336	0.90740
2.20	0.10577	0.93214
2.40	0.07768	0.95034
2.60	0.05690	0.96370
2.80	0.04163	0.97347
3.00	0.03043	0.98062
3.20	0.02224	0.98584
3.40	0.01625	0.98965
3.60	0.01187	0.99244
3.80	0.00867	0.99448
4.00	0.00633	0.99597
4.20	0.00462	0.99705
4.40	0.00338	0.99785
4.60	0.00247	0.99842
4.80	0.00180	0.99885
5.00	0.00132	0.99916

Table I (Cont.)

$\frac{k}{h} = 1.5$

$\frac{y}{h}$	$\frac{E}{V_o/h}$	$\frac{V}{V_o}$
0.00	0.48916	0.00000
0.20	0.48925	0.09784
0.40	0.48911	0.19569
0.60	0.48737	0.29338
0.80	0.48150	0.39036
1.00	0.46770	0.48545
1.20	0.44151	0.57662
1.40	0.40000	0.66103
1.60	0.34478	0.73568
1.80	0.28269	0.79847
2.00	0.22231	0.84888
2.20	0.16970	0.88793
2.40	0.12711	0.91744
2.60	0.09414	0.93942
2.80	0.06928	0.95564
3.00	0.05081	0.96755
3.20	0.03719	0.97628
3.40	0.02720	0.98267
3.60	0.01988	0.98734
3.80	0.01452	0.99075
4.00	0.01061	0.99324
4.20	0.00775	0.99506
4.40	0.00566	0.99639
4.60	0.00414	0.99736
4.80	0.00302	0.99807
5.00	0.00221	0.99859

Table I (Cont.)

$\frac{k}{h} = 2.0$

$\frac{y}{h}$	$\frac{E}{V_o/h}$	$\frac{V}{V_o}$
0.00	0.37823	0.00000
0.20	0.37887	0.07569
0.40	0.38072	0.15163
0.60	0.38353	0.22804
0.80	0.38674	0.30507
1.00	0.38936	0.38270
1.20	0.38966	0.46066
1.40	0.38492	0.53823
1.60	0.37151	0.61405
1.80	0.34596	0.68602
2.00	0.30731	0.75155
2.20	0.25912	0.80830
2.40	0.20831	0.85502
2.60	0.16142	0.89189
2.80	0.12203	0.92010
3.00	0.09087	0.94126
3.20	0.06708	0.95695
3.40	0.04928	0.96849
3.60	0.03610	0.97696
3.80	0.02641	0.98316
4.00	0.01931	0.98770
4.20	0.01411	0.99101
4.40	0.01031	0.99343
4.60	0.00753	0.99520
4.80	0.00550	0.99649
5.00	0.00402	0.99744

Table I (Cont.)

$\frac{k}{h} = 2.5$

$\frac{y}{h}$	$\frac{E}{V_o/h}$	$\frac{V}{V_o}$
0.00	0.30581	0.00000
0.20	0.30636	0.06120
0.40	0.30799	0.12262
0.60	0.31067	0.18446
0.80	0.31431	0.24694
1.00	0.31872	0.31024
1.20	0.32357	0.37446
1.40	0.32818	0.43965
1.60	0.33137	0.50565
1.80	0.33119	0.57198
2.00	0.32478	0.63771
2.20	0.30885	0.70125
2.40	0.28125	0.76046
2.60	0.24321	0.81304
2.80	0.19978	0.85738
3.00	0.15726	0.89302
3.20	0.12011	0.92065
3.40	0.08998	0.94154
3.60	0.06665	0.95710
3.80	0.04906	0.96859
4.00	0.03598	0.97702
4.20	0.02634	0.98320
4.40	0.01926	0.98773
4.60	0.01408	0.99103
4.80	0.01029	0.99345
5.00	0.00751	0.99521

Table I (Cont.)

$\frac{k}{h} = 3.0$

$\frac{y}{h}$	$\frac{E}{V_o/h}$	$\frac{V}{V_o}$
0.00	0.25301	0.00000
0.20	0.25341	0.05063
0.40	0.25459	0.10142
0.60	0.25658	0.15252
0.80	0.25936	0.20410
1.00	0.26293	0.25631
1.20	0.26727	0.30932
1.40	0.27226	0.36326
1.60	0.27772	0.41826
1.80	0.28324	0.47436
2.00	0.28805	0.53151
2.20	0.29084	0.58945
2.40	0.28950	0.64758
2.60	0.28119	0.70478
2.80	0.26320	0.75940
3.00	0.23470	0.80935
3.20	0.19844	0.85275
3.40	0.15983	0.88858
3.60	0.12399	0.91688
3.80	0.09380	0.93856
4.00	0.06987	0.95482
4.20	0.05159	0.96688
4.40	0.03790	0.97576
4.60	0.02777	0.98228
4.80	0.02032	0.98705
5.00	0.01485	0.99054

Table I (Cont.)

$\frac{k}{h} = 3.5$

$\frac{y}{h}$	$\frac{E}{V_o/h}$	$\frac{V}{V_o}$
0.00	0.21623	0.00000
0.20	0.21651	0.04326
0.40	0.21736	0.08664
0.60	0.21879	0.13025
0.80	0.22082	0.17420
1.00	0.22346	0.21862
1.20	0.22672	0.26362
1.40	0.23062	0.30934
1.60	0.23515	0.35591
1.80	0.24027	0.40345
2.00	0.24586	0.45205
2.20	0.25163	0.50180
2.40	0.25708	0.55269
2.60	0.26124	0.60455
2.80	0.26255	0.65699
3.00	0.25866	0.70922
3.20	0.24689	0.75993
3.40	0.22545	0.80732
3.60	0.19534	0.84952
3.80	0.16067	0.88516
4.00	0.12658	0.91384
4.20	0.09672	0.93608
4.40	0.07248	0.95291
4.60	0.05370	0.96544
4.80	0.03952	0.97469
5.00	0.02899	0.98149

II. COMPUTER RESULTS FOR PARTICLE TRAJECTORIES

A. Cyclotron Units

Output data from the computer programs to be described in this report are all in cyclotron units except for the kinetic energy (E_k) which is in Mev. The unit of magnetic field, b, is given as

$$b = \frac{m_o \omega}{e}$$

where $\omega = 2\pi\nu_o$ with ν_o the frequency of the r-f system, m_o and e are the rest mass and charge of the particle (in this case the proton). Therefore, b is the value of the isochronous magnetic field at r = 0. The cyclotron length unit, a, is determined as

$$a = \frac{c}{\omega},$$

where c is the speed of light; therefore, $ba = \frac{m_o c}{e}$. For the fields under consideration b = 13.6 kilogauss is the cyclotron magnetic field unit; therefore, the cyclotron length unit is given by a = 90.4". All magnetic fields and lengths used in this report are expressed in terms of b and a and are called cyclotron units (abbreviated "c.u."). All momenta (e.g. p_x and p_y) in this report are given in units of $m_o c$.

From the cyclotron units defined above, then it follows that the electric field cyclotron unit is $bc = \frac{m_o c^2}{ea}$. Therefore, the potential is given in units of $\frac{m_o c^2}{e}$. The magnitude of the potential is chosen such that $4eV_o = \delta = 0.0003$, where δ is the energy gain per turn. For the proton case ($m_o c^2 = 938.23$ Mev) δ is then 281.5 Kev. Similarly, the electric field cyclotron unit is 10.4 Mv/in.

B. Cartwheel Code

Charged particles moving in a cyclotron are subject to the well-known Lorentz force

$$\mathbf{F} = \frac{d\mathbf{P}}{dt} = q\,[\mathbf{E} + (\mathbf{v} \times \mathbf{B})] \tag{2.1}$$

where q is the charge on the particle, E is the electric field produced by the dees, v is the velocity of the particle and B is the magnetic field. The MISTIC computer program Cartwheel determines the median plane orbit of a particle subject to the Lorentz force. It must be emphasized that the Cartwheel Code considers only single particle orbits as no inter-particle interaction is considered.

The time-varying electric field is chosen

$$\mathbf{E}(r,t) = \mathbf{E}(r) \cos \omega\,(t + t_o), \tag{2.2}$$

where E(r) is the amplitude of the electric field and ω is the radian

frequency of the r-f system. The factor t_o has been introduced to take account of particles starting at different times of the voltage cycle. For the median plane case $E(r) = E_x + E_y$; therefore, the desired equations of motion from Eq. (2.1) for the median plane are

$$\frac{dP_x}{dt} = q\left[E_x \cos\omega(t+t_o) - v_y B_z\right], \tag{2.3a}$$

$$\frac{dP_y}{dt} = q\left[E_y \cos\omega(t+t_o) + v_x B_z\right], \tag{2.3b}$$

where $B = -B_z$ $(z = 0)$.

For Cartwheel the magnetic field is calculated from a set of first harmonic Fourier coefficients [7] by the equation

$$B_z(r\theta) = B_o(r) + H_1(r)\cos 3\theta - G_1(r)\sin 3\theta. \tag{2.4}$$

The term $B_o(r)$ is the average field at a given radius, and the last two terms are the harmonic flutter field. For the calculations herein, the magnetic field used is designated as B26.3A which is a reasonably well isochronized three-sector field characterized by a high flutter field with weak spiral. B26.3A is a re-isochronized version of B26.29A [8].

If the quantities of Eqs. (2.3) are expressed in dimensionless form by means of cyclotron units, the resultant equations are

$$\frac{dP_x}{dt} = E_x \cos(t + t_o) - v_y B_z,$$

$$\frac{dP_y}{dt} = E_y \cos(t + t_o) + v_x B_z.$$

For further calculation consider the relativistic equation for momentum,

$$P_x = \frac{m_o v_x}{\sqrt{1 - v^2/c^2}} .$$

If again these quantities are expressed in terms of cyclotron units, the result is

$$P_x = \frac{v_x}{\sqrt{1 - v^2}} .$$

Therefore, it follows that $[1 - v^2]^{-1} = [1 + P^2]$ in these relativistic cyclotron units. The velocity may then be determined

$$v_x = \frac{P_x}{\sqrt{1 + P^2}} ,$$

$$v_y = \frac{P_y}{\sqrt{1 + P^2}} .$$

Similarly, to calculate the kinetic energy (E_k) of a particle, consider the relativistic expression for total energy (mc^2) associated with a moving mass

$$mc^2 = E_k + m_o c^2,$$

where $m_o c^2$ is the rest energy of the mass. Solving this equation for E_k and applying the relation above connecting velocity and momentum, the result is

$$E_k = (\sqrt{1 + P^2} - 1)\, m_o c^2,$$

where P is measured in cyclotron units. The Cartwheel Code numerically integrates the equations of motion as summarized below.

$$\frac{dP_x}{dt} = E_x \cos(t+t_o) - v_y B_z,$$

$$\frac{dP_y}{dt} = E_y \cos(t+t_o) + v_x B_z,$$

$$\frac{dx}{dt} = v_x, \quad \frac{dy}{dt} = v_y, \tag{2.5}$$

$$v_x = \frac{P_x}{\sqrt{1+P^2}}, \quad v_y = \frac{P_y}{\sqrt{1+P^2}},$$

$$E_k = (\sqrt{1+P^2} - 1)\, m_o c^2.$$

The Cartwheel Code will give results for the quantities x, y, P_x, P_y and E_k at a time t which is a desired multiple of the fixed time interval.

C. Central Cyclotron Orbits

In this section results will be presented and compared for various electric and magnetic field configurations. As an introduction to orbit determinations, consider the motion of a particle in a uniform magnetic field and the electric field within the dee gap as uniformly produced by two parallel plates. Therefore, the electric field is determined by $E_y = E_o f(y)$ where $f(y) = 1$ for $-k \leq y \leq k$ and $f(y) = 0$ elsewhere. For the uniform magnetic field Eq. (2.4) reduces to $B_z(r, \theta) = B_o$ is a constant. Using these determinations for the electric and magnetic fields and specifying that at $t = 0$ the particle is at rest at the origin, the Cartwheel Code then determines the orbit for the first two revolutions as shown in Fig. 2-1 with the parallel plate electric field between $\pm .015$ c.u. This value was chosen as the electric field falls off roughly in $k + h$ (Fig. 1-1). This type of initial conditions is roughly analogous to the open arc injection system.

For this simple field arrangement it is possible to integrate directly the equations of motion (Eqs. 2-5) in the non-relativistic approximations. The resultant equations for this integration are

$$x = x_o + \frac{E_y}{2} (t\cos t - \sin t) + v_{x_o} \sin t + v_{y_o} \cos t - v_{y_o}, \tag{2.6a}$$

$$y = y_o + \frac{E_y}{2} (t \sin t) + v_{y_o} \sin t - v_{x_o} \cos t + v_{x_o}. \tag{2.6b}$$

The case of parallel plate electric field and uniform magnetic field is a simple case that can be calculated directly, and this direct method is used to check the Cartwheel Code operation and set a basis for study of other fields.

The tabulation below compares values obtained from the direct calculation and from Cartwheel.

	Direct Calculation			Cartwheel		
t	x	y	E_k(Kev)	x	y	E_k(Kev)
$\pi/6$	-00011637	+00065450	2.9	-00011638	+00065449	2.9
$\pi/2$	-00250000	+00392699	10.2	-00249996	+00392695	10.2
π	-00785398	00000000	28.9	-00785389	+00000019	28.9
2π	+01570796	00000000	115.7	+01570754	-00000304	115.7
3π	-02308448	+0044228	238.1	-02308398	+00044235	238.3

The error in the direct calculations is that $\sqrt{1 + P^2}$ has been set equal to unity; that is, relativistic effects have been neglected. Therefore, the disagreement of values given above should be of order $\frac{E_k}{m_o c^2}$; this error is in agreement with the values given. For example, for the values at $t = 2\pi$ the error in x is of order 10^{-5}. For this t value $\frac{E_k}{m_o c^2} = \frac{.1157}{938.2} \cong 10^{-5}$. Therefore, the agreement appears to be qualitatively correct.

In order to investigate the effects on the orbit due to three sector magnetic field, Cartwheel is used to determine the first two revolutions of the orbit as above but now using the B26. 3A magnetic field. The resultant orbit is shown in Fig. 2-2, where the radial lines locate the magnetic field hills and the parallel plate electric field is between $\pm$. 015 c. u. The results listed below tabulate Cartwheel results for comparison of the two magnetic fields both with the parallel plate electric field.

	B (uniform)			B26. 3A		
t	x	y	E_k(Kev)	x	y	E_k(Kev)
$\pi/6$	-00011638	+00065449	2. 9	-00011638	+00065449	2. 9
$\pi/2$	-00249996	+00392695	10. 2	-00250038	+00392647	10. 2
π	-00785389	+00000019	28. 9	-00785276	-00000552	29. 0
2π	+01570754	-00000304	115. 7	+01574338	-00001071	115. 7
3π	-02308398	+00044235	238. 3	-02296333	+00048347	238. 2

It is difficult to estimate the effect on the orbit due to the non-uniform magnetic field. Nevertheless, close agreement is expected for the central region (x, y < . 01 c. u.), as the three sector field is essentially

uniform in this region. Listed below are the values of B_o, H_1 and G_1 in Eq. (2.4) for the first five r values.

r	B_o	H_1	G_1
0	1.0000000	0000000	0000000
Δr	1.0000392	.0018224	-.0002800
$2\Delta r$	1.0001088	.0044156	-.0073764
$3\Delta r$	1.0001452	.0137724	-.0221864
$4\Delta r$	1.0000380	.0277704	-.0418504

where Δr = .008092404 c.u.

To compare the effects on the orbit of the parallel plate electric field with the electric field derived in Sec. I-C, Cartwheel is used to determine the orbit for the first two revolutions as shown in Fig. 2-3. For comparison the orbit in the uniform magnetic field and parallel plate electric field is also shown as a dashed line. In this determination the dee electric field is used with B26.3A magnetic field. The radial lines locate the magnetic field hills, and the dee gap is between $\pm$.005 c.u. For this case the electric field is determined such that k/h = 0.5; hence h = .01 c.u. Fig. 2-4 shows the shape of the dee electric field in comparison with the parallel plate electric field used above. The potential is normalized so that the difference in potential

between $+\infty$ and $-\infty$ is the same for both electric fields. Cartwheel results for the two electric fields with B26. 3A magnetic field for both cases are presented below.

	Parallel plate field			Derived field		
t	x	y	E_k(Kev)	x	y	E_k(Kev)
$\pi/6$	-00011638	+00065449	2.9	-00015191	+00085412	4.9
$\pi/2$	-00250038	+00392647	10.2	-00324390	+00506155	16.6
π	-00785276	-00000552	29.0	-01029964	+00038897	44.0
2π	+01574338	-00001071	115.7	+01768538	-00092169	141.0
3π	-02296333	+00048347	238.2	-02384708	+00137340	257.6

Since the dee electric field is stronger near the x axis and the phase difference is small, it is expected that the particle will gain energy at a faster rate in this region.

If the non-relativistic expressions as integrated, Eqs. (2.6), are used to determine the position of the particle assuming uniform magnetic field and using the value of the derived electric field as given at y = 0 from Fig. 2-4, these directly calculated results agree with output data from Cartwheel as tabulated below.

	Calculated		Cartwheel	
t	x	y	x	y
$2\pi/48$	-00000244	+00005576	-00000244	+00005576
$2\pi/24$	-00001939	+00022119	-00001939	+00022113

The error is expected since it was assumed that the maximum electric field is uniform, and examination of Fig. 2-4 shows that the electric field is not uniform for this region.

The results tabulated below present the phase difference ($\phi = t - \theta$) and energy at the end of each half revolution in time for the orbit determinations corresponding to the parallel plate electron field and the derived electron field both with B26.3A magnetic field.

	Parallel plate field		Derived field	
t	ϕ	E_k(Kev)	ϕ	E_k(Kev)
π	-0° 2.5'	29.0	$+2^\circ$ 10'	44.0
2π	$+0^\circ$ 2.5'	115.7	$+2^\circ$ 59'	141.0
3π	$+1^\circ$ 12'	238.2	$+3^\circ$ 18'	257.6
4π	$+1^\circ$ 12'	369.4	$+3^\circ$ 0'	383.6

The difference in phase per revolution will be zero if the magnetic field is isochronous and the particle starts from rest at the origin. However, the magnetic field is isochronous only for the equilibrium orbit. The more the actual orbit deviates from the equilibrium orbit or the more the actual orbit becomes off-center with respect to the origin, the phase difference will then increase. Since non-zero phase difference occurs as presented in the tabulation, it is concluded that the orbits are off center with respect to the origin. The phase difference is still quite small and is not an important factor. The phase difference property will be discussed further in the next section.

D. Particle Source Location

In this section investigations are considered which affect the initial position of the particle. By far the most stringent condition on the initial position arises in connection with orbit stability in phase space [9, 10]. Fig. 2-5 shows the stability region at an energy of 2.5 Mev at $\theta = 0$. This energy is chosen for the reason that if the point in phase space defined by the particle is within the stable region at this energy, it will generally remain within the

stable region at higher energies. However, the stable region expands quite rapidly as the energy increases, therefore, a particle which is outside the stable region at a low energy could be within the stable region at a higher energy.

In order to determine the phase space point for the accelerated ions, the Cartwheel Code is used to determine the position and momentum at the energy corresponding to the stable region. Five Cartwheel determinations were made in this manner all for the case of the dee electric field and B26. 3A magnetic field. The five determinations correspond to five different starting positions as shown in Fig. 2-5. The Cartwheel output is interpolated to determine r and P_r at $\theta = 0$. The tabulation below summarizes the result of this interpolation; the results correspond to ten completed revolutions.

Starting position	E_k(Mev)	ϕ	r	P_r
Origin	2. 583	2^o 11'	+07719091	+00543734
+0. 003	2. 584	3^o 36'	+08098156	+00369580
+0. 006	2. 585	5^o 11'	+08900653	+00079326
-0. 003	2. 583	1^o 15'	+07473902	+00624852
-0. 006	2. 583	1^o 12'	+07259057	+00600750

The phase space point determined by r and P_r is investigated relative to the stable region. Examination of Fig. 2-5 shows that the acceptability of the particle phase space point within the stable region is dependent on the starting position. Protons starting from positions corresponding to 1, 4 or 5 are within the stable region and are suitable for further acceleration, while protons starting from positions corresponding to 2 and 3 are outside the stable region and may be lost for further use due to radial instability. From the values at E_k in the tabulation above, it is seen that the kinetic energy is relatively insensative to starting position. This is to be expected since the electric field is independent of the value of x and the magnetic field is isochronous. The phase slip remains relatively small due to the isochronous magnetic field.

Stability can be explained qualitatively on the basis of orbit centering. If the orbit is badly off center, the phase space point determined as above will generally be outside the stable region. Examination of Fig. 2-5 shows that the orbits corresponding to initial conditions 1, 4 and 5 are closely centered while those of 2 and 3 are more off center.

In the Cartwheel determinations above, information on the phase slip at the end of each successive revolution is also obtained. The position of the particle at the time of maximum electric field

for a total of ten r-f cycles is shown in Fig. 2-6. If the particle orbit frequency were exactly the same as the r-f oscillation frequency, the particle would be on the x-axis at the time of maximum electric field. The three curves of Fig. 2-6 correspond to three of the five starting positions above: one starting at the origin, the next displaced Δx = +. 006 c. u. along the x-axis, and the third starting with an x displacement of Δx = -. 006 c. u. These three values were chosen because they exhibit the maximum characteristics. It is important to observe that the phase difference is remaining relatively small and is not accumulating at a rapid rate.

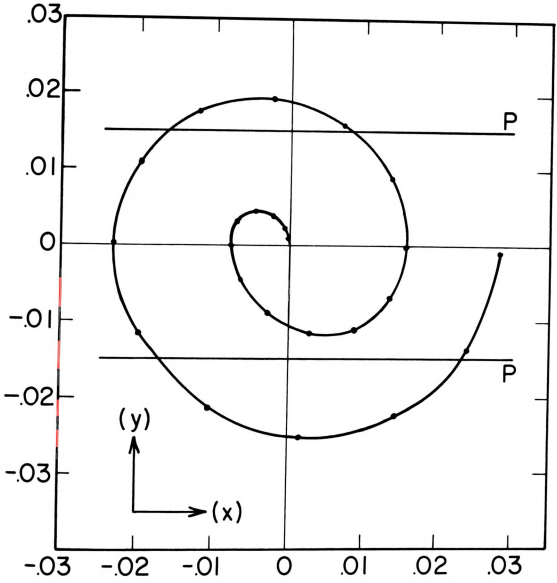

Fig. 2-1. Proton Orbit for First Two Revolutions in Parallel Plate Electric Field and Uniform Magnetic Field, Sec. C. "P" denotes position of parallel plates; x and y in cyclotron units. Points on curve denote steps of 30° in time.

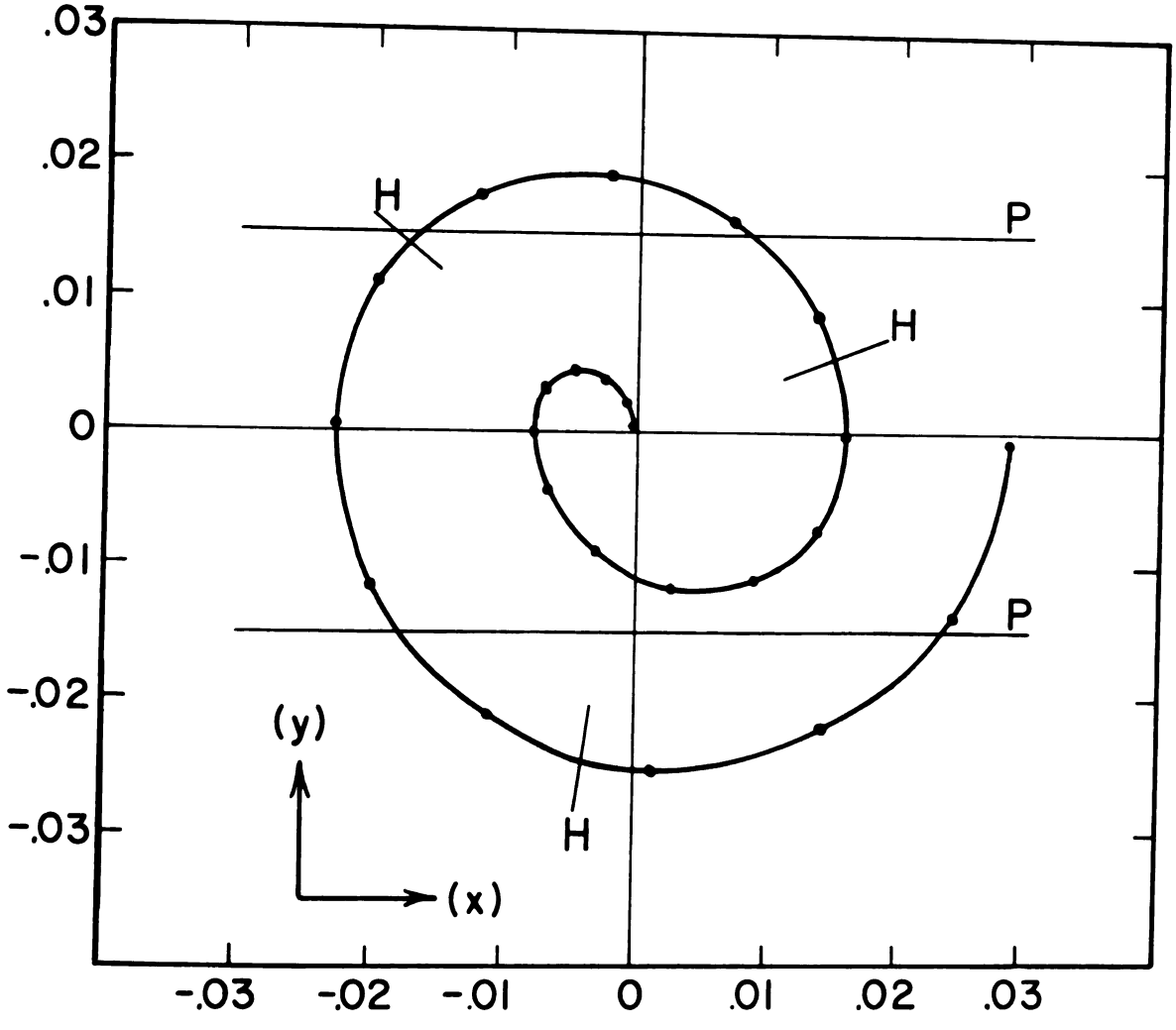

Fig. 2-2. Proton Orbit for First Two Revolutions in Parallel Plate Electric Field and B26.3A Magnetic Field, Sec. C. "P" denotes position of parallel plates; x and y in cyclotron units. Points on curve denote steps of 30° in time. "H" denotes magnetic field hills.

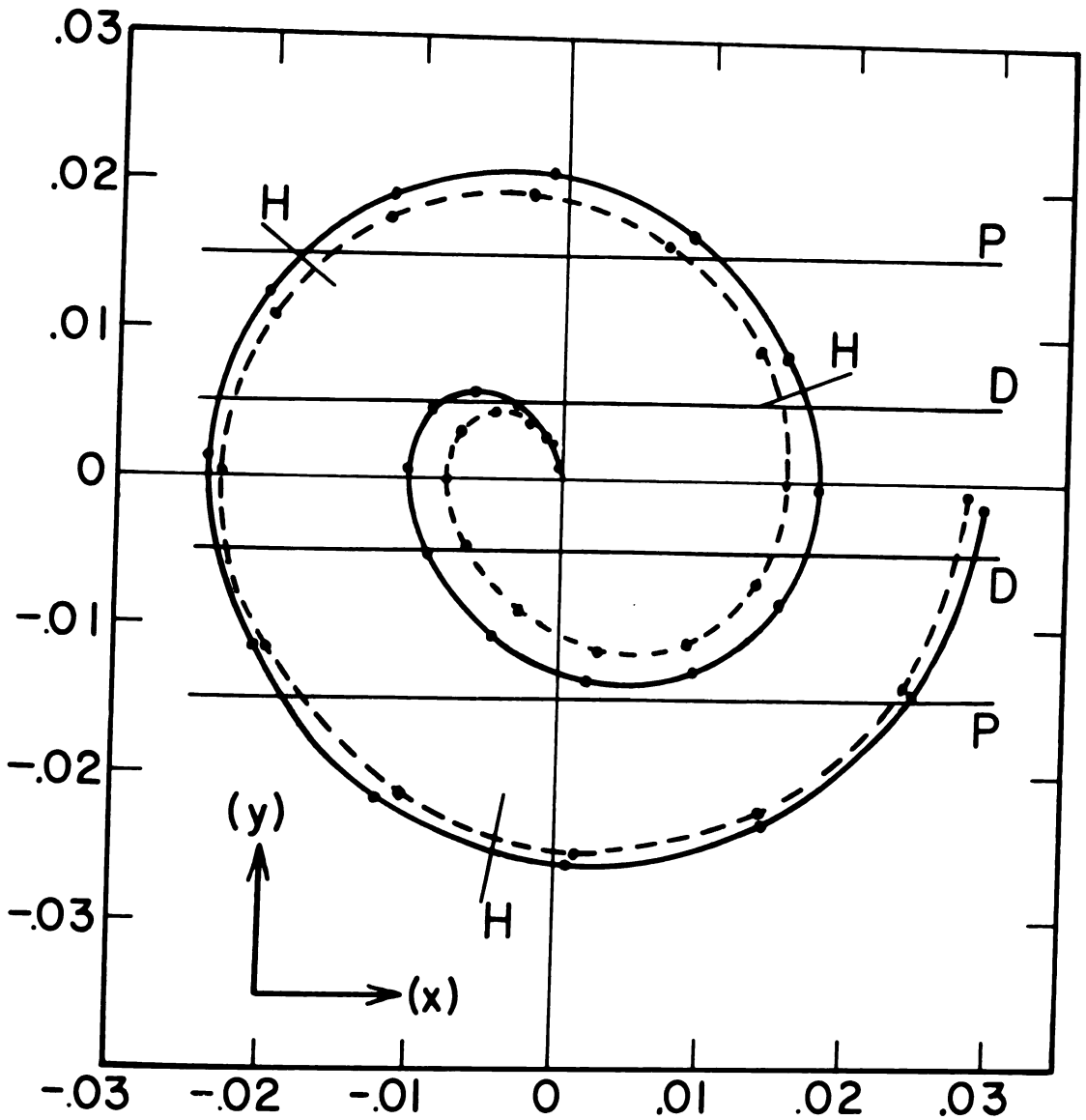

Fig. 2-3. Proton Orbit for First Two Revolutions in Derived Electric Field and B26.3A Magnetic Field, Sec.C. "D" denotes edge of dees; "H" denotes magnetic field hills. Points on curve denote steps of 30° in time; x and y in cyclotron units. Fig. 1-1 superimposed as dashed line for comparison.

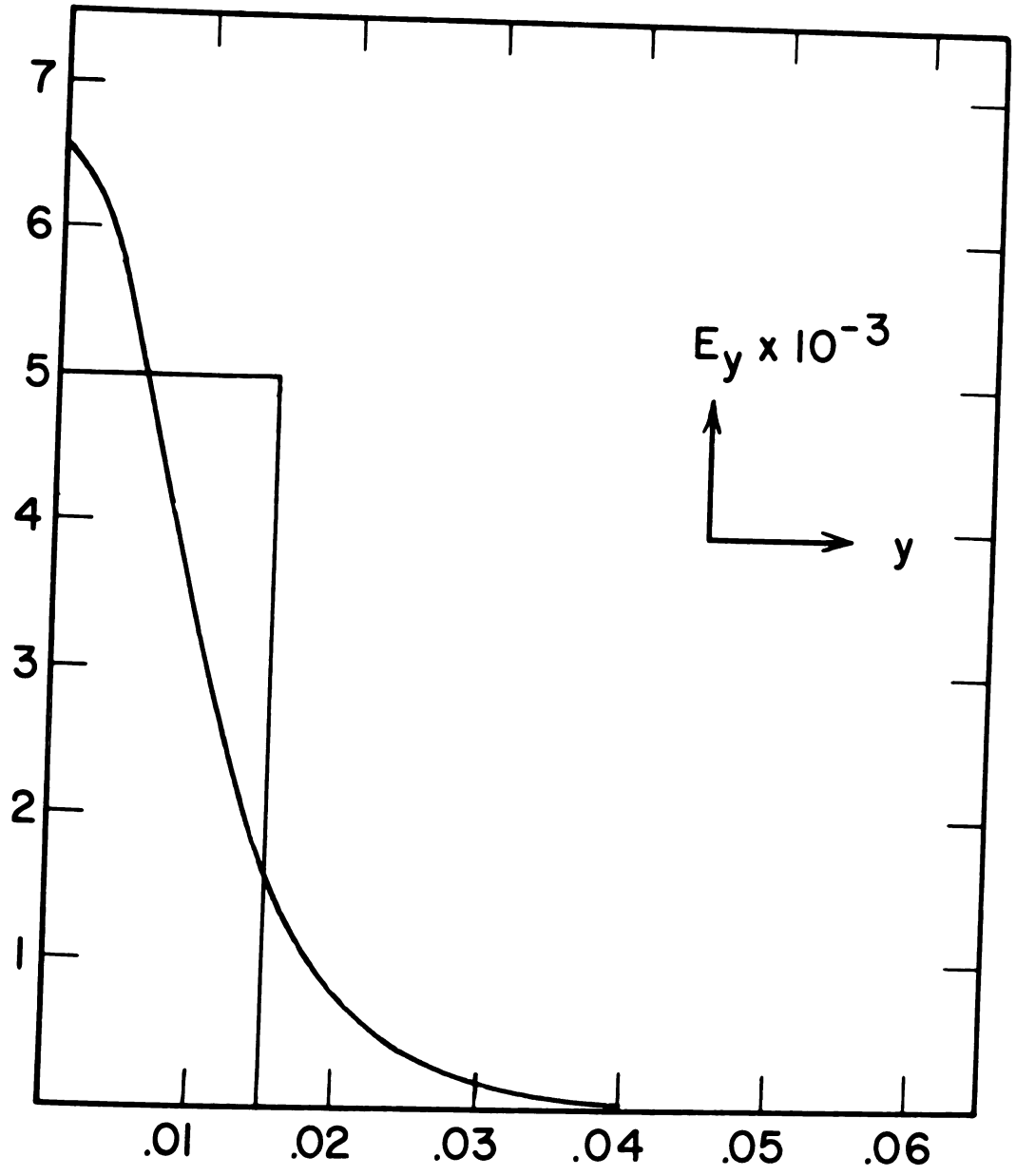

Fig. 2-4. Comparison of Parallel Plate and Derived Electric Fields; E and y in cyclotron units, Sec. C.

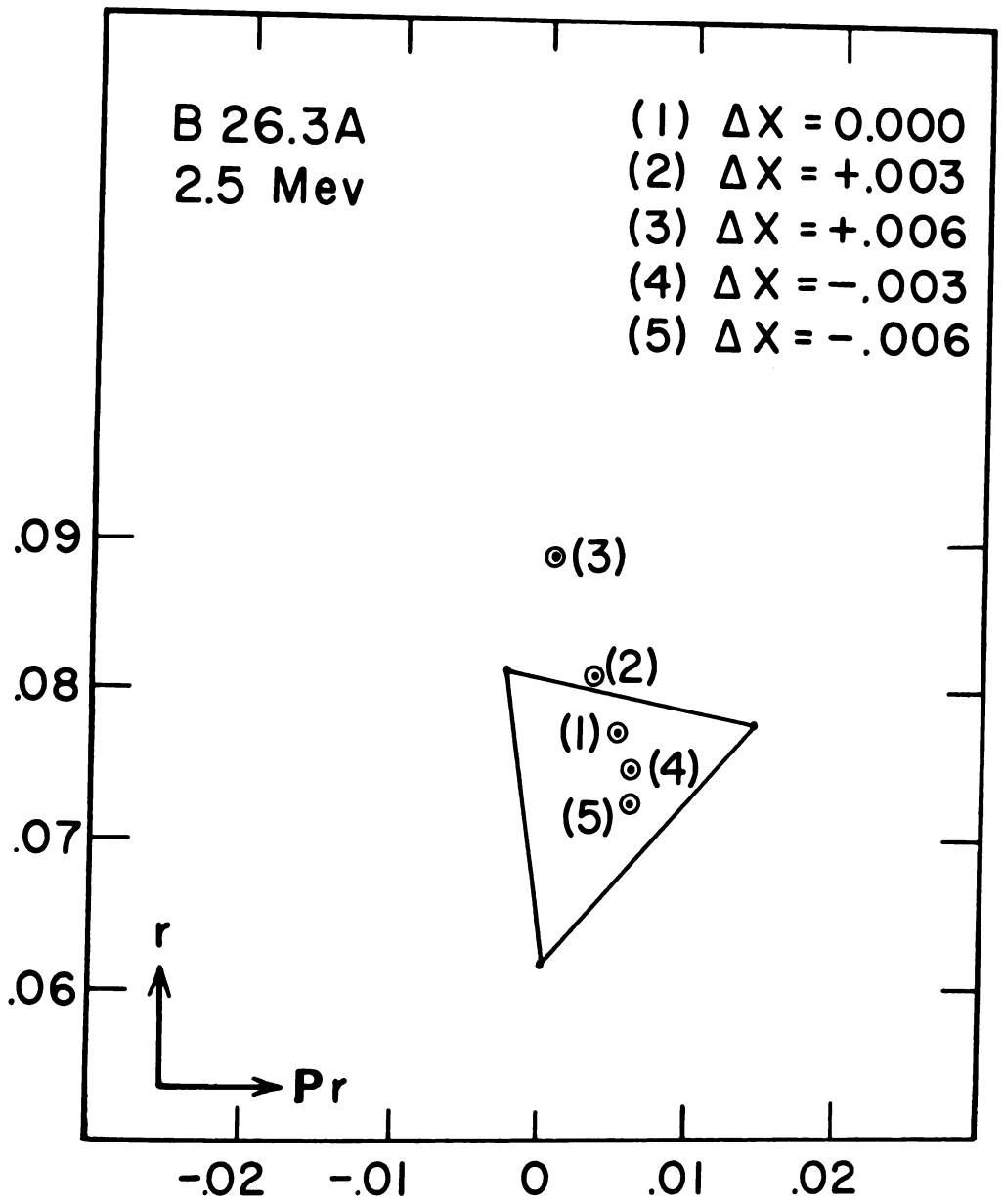

Fig. 2-5. Stability Region (2.5 Mev) at θ=0 and Phase Space Points Associated with Accelerated Particles for Various Starting Positions for Derived Electric Field and B26.3A Magnetic Field. r and P_r in cyclotron units.

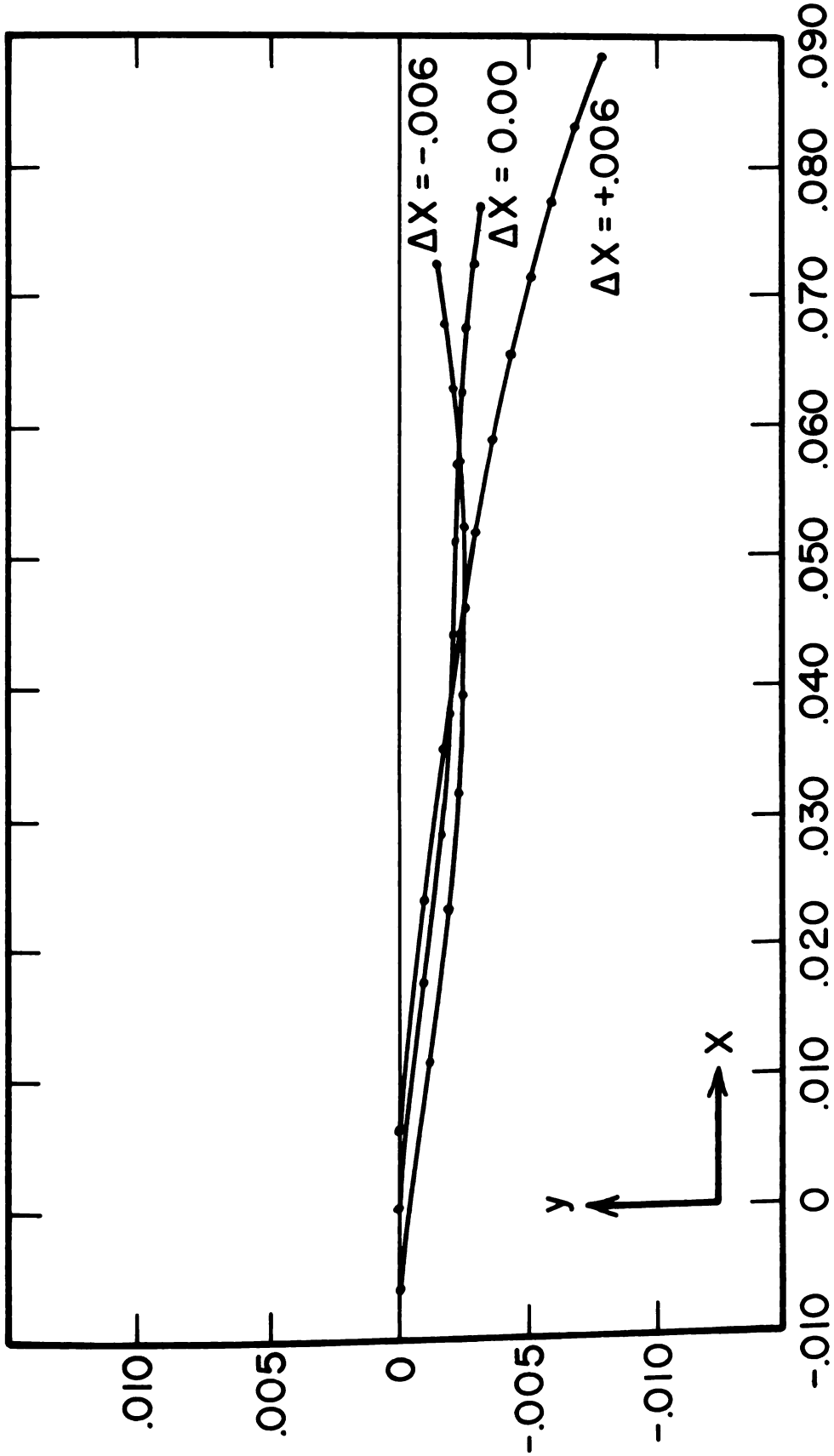

Fig. 2-6. Particle Phase Slip at the End of Each of Ten Successive Revolutions for Three Starting Positions. x and y in cyclotron units, Sec. D.

BIBLIOGRAPHY

[1] Robert R. Wilson, Physical Review 53 (1938), pp. 408-420.

[2] M. E. Rose, Physical Review 53 (1938), pp. 392-408.

[3] D. Bohm and L. L. Foldy, Physical Review 72 (1947), pp. 649-661.

[4] R. L. Murray and L. T. Ratner, Journal of Applied Physics 24 (1953), pp. 67-69.

[5] T. I. Arnette, unpublished.

[6] R. V. Churchill, Complex Variables and Applications (McGraw-Hill Book Company, Inc., New York, 1960), pp. 220-228.

[7] H. G. Blosser and D. A. Flanigan, MSUCP-5 (Michigan State University Publication, October 1960).

[8] M. M. Gordon and W. S. Hudec, MSUCP-11 (Michigan State University Publication, November 1961), pp. 13-34.

[9] M. M. Gordon and T. A. Welton, Nuclear Instruments and Methods 6 (No. 3, 1960), pp. 221-233.

[10] J. E. Stover, MSUCP-3 (Michigan State University Publication, August 1960), pp. 27-42.